Theoretical Study of Reaction Mechanisms for NCX (X = O, S) + C_2H_2

Hsin-Tsung Chen and Jia-Jen Ho*

Department of Chemistry, National Taiwan Normal University, 88, Section 4, Tingchow Road, Taipei, Taiwan 117

Received: December 17, 2002; In Final Form: April 29, 2003

The reaction mechanisms for NCX (X = O, S) with C_2H_2 was studied theoretically. The possible reaction mechanisms of NCO + C_2H_2 investigated in this study were categorized into five different pathways leading to the five possible final products: HCCO + HCN, HCCO + HNC, HNCO + C_2H, HONC + C_2H, and HC_2NCO + H, labeled in order from P1 to P5, respectively. Similar calculations were also carried out for the NCS counterpart, and the energy barriers as well as the products were compared. Direct hydrogen abstraction is favored in the formation of HNCO instead of HOCN. In contrast, it is much easier to form HSCN rather than HNCS. There are two different paths for the oxazole/thiazole formation as an intermediate, and the order of energy barriers of these two paths is opposite in NCO and NCS. The product channel of HNCO/HSCN + C_2H may be kinetically favored at higher temperature. Other product channels are consistent with the experimental prediction of the formation of initial short-lifetime NCO/NCS−C_2H_2 adducts which then undergo rapid transformation into the products.

Introduction

The kinetics of nitrogen-containing radicals (NCX, X = O, S) in the gas phase are of great interest because of the role these species play in the formation and removal of NO_x pollutants in combustion processes.[1] For example, the isocyanate radical, NCO, plays a key intermediate in combustion. Several experimental studies have demonstrated that NCO reacts quickly with NO,[2−10] forming N_2O + CO and N_2 + CO_2 products, and with NO_2,[7,8,11,12] forming N_2O + CO_2. Theoretical studies of NCO + NO and NCO + OH have been reported.[13,14] In contrast, very little is known about the mechanism and kinetics of NCO reactions with hydrocarbons,[15−20] especially, about the reactions of NCO with unsaturated hydrocarbons, which are probably important in fuel-rich combustion. Reactions of NCO radicals with saturated hydrocarbons have been investigated in the temperature range 294−1113 K by Schuck et al.[18] And the reaction with C_2H_2 was studied over wide pressure and temperature ranges using a pulsed UV excimer laser photolysis (LP)/laser-induced fluorescence (LIF) technique by Wiesen et al.[19] The proposed reaction channels were the following:

$$NCO + C_2H_2 \rightarrow HCCO + HCN \quad (A)$$

$$HCCO + HNC \quad (B)$$

$$HNCO + C_2H \quad (C)$$

$$NCOH + C_2H \quad (D)$$

$$HCCNCO + H \quad (E)$$

Park and Hershberger[16] observed that the hydrogen abstraction to form HNCO + alkyl radicals (the (C) path) was a major product channel for NCO reacting with most of the saturated hydrocarbons and C_2H_2, but not for C_2H_4. For example, from their observation, with C_4H_{10}, the relative HNCO formed was 1.0, and with the unsaturated acetylene, C_2H_2, 0.19, whereas with C_2H_4, very little HNCO (only 0.04). They suggested the formation of a complex when NCO reacted with these unsaturated hydrocarbons (especially C_2H_4), which could be stabilized by collision with a third body. This idea was also supported by Perry[17] in which he proposed that NCO first added across the double bond, and the resulting complex was then either stabilized by a third-body collision, or underwent H atom elimination, the so-called addition−elimination mechanism. Meanwhile, Wiesen et al.[19] proposed another possible mechanism which led to the formation of HCCO + HCN via a 1,3-H shift of a five-membered cyclic complex, oxazole. The proposed intermediate oxazole complex possesses aromatic character resulting from six delocalized π electrons.

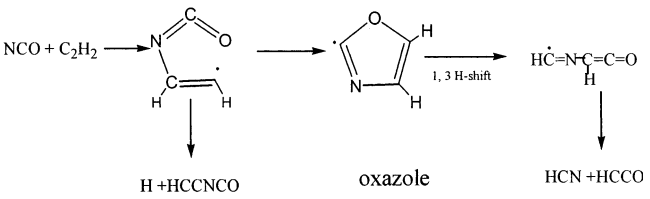

In this paper, we report the possible reaction pathways of NCO radicals with C_2H_2 by a theoretical method. A similar reaction by using the NCS counterpart was also studied. A quantum mechanical calculation using the density functional theory (DFT) and the coupled cluster method (CCSD(T)) was performed.

Calculation Method

We carried out the ab initio molecular orbital calculations by using the Gaussian-98 program package.[21] The stationary points on the potential energy surfaces were optimized mainly by density functional theory with the Becke three-parameter hybrid method and the Lee−Yang−Parr correlation functional approximation (B3LYP).[22−23] Basis sets with increasing ac-

* Corresponding author. Phone: (886)-2-29309085. Fax: (886)-2-29324249. E-mail: jjh@scc.ntnu.edu.tw.

10.1021/jp022613z CCC: $25.00
Published on Web 08/15/2003

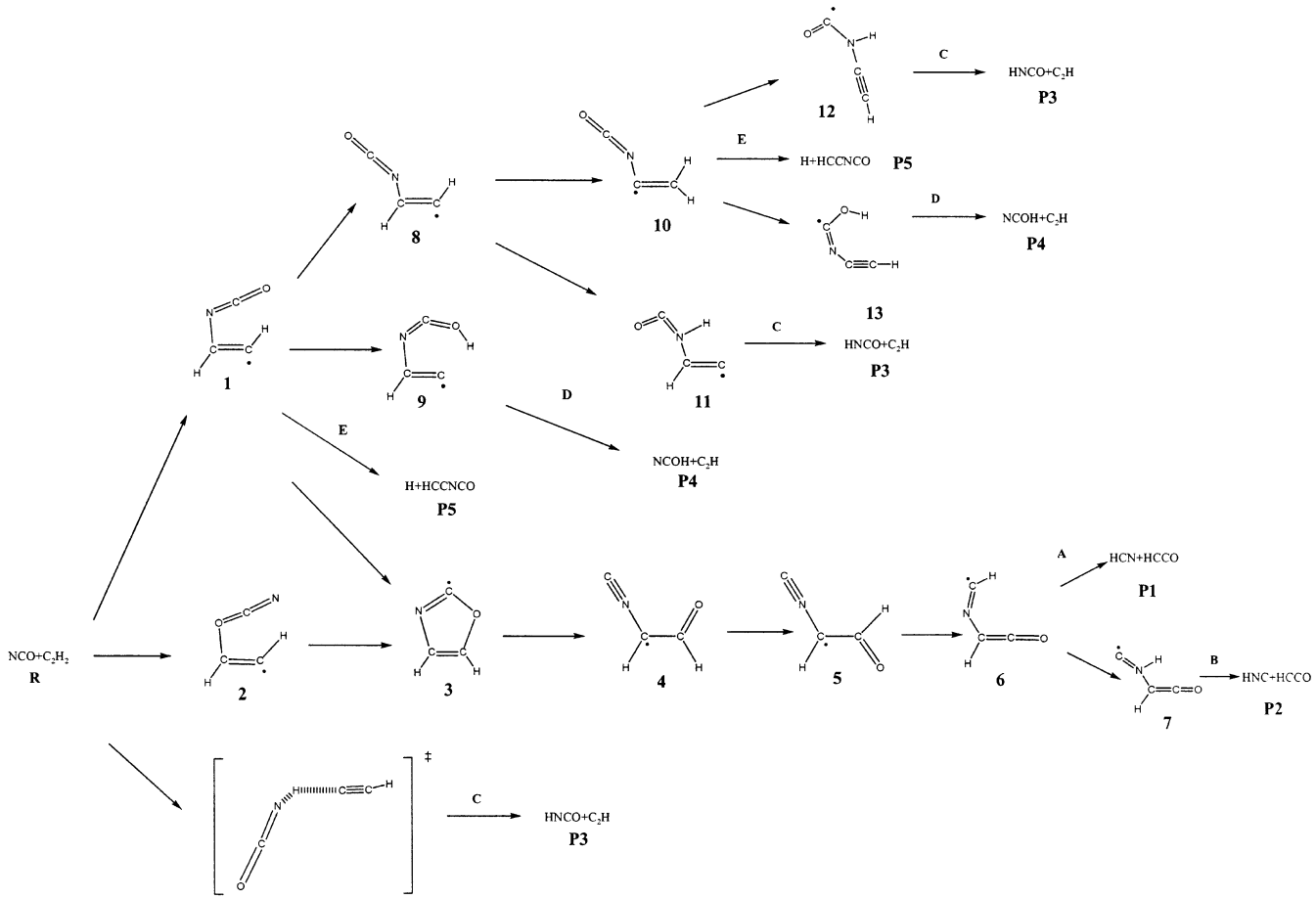

Figure 1. The possible reaction pathways of NCO + C_2H_2 are characterized into five different parts: A, B, C, D, and E.

curacy of polarized split-valence and diffuse functions for heavy and hydrogen atoms 6-31++G** were used in the calculations. Vibrational analysis was carried out at the same level of theory to characterize the optimized structures as local minima or transition states. A zero-point energy (ZPE) correction was considered. An intrinsic reaction coordinate (IRC)[24] calculation was also performed to confirm the connection between the transition state and the intermediates. To obtain more reliable energies, coupled cluster calculations with single and double excitations and an evaluation by perturbation theory of triple contributions CCSD(T)[25] were carried out for those geometries optimized at the B3LYP/6-31++G** level, denoted as CCSD(T)/6-31++G**//B3LYP/6-31++G**. The energy is corrected with ZPE at B3LYP/6-31++G** level. The reason that we adopted this level and basis set was that we applied it to calculate the activation energy of a similar reaction of NCO + C_2H_6 → HNCO + C_2H_5, and it yielded a satisfactory result (3.68 kcal/mol, or 15.38 kJ/mol) in good agreement with the experimental data (15.2 ± 0.4 kJ/mol).[26] Therefore, we are confident with the data calculated at this level for this type of reaction.

Results and Discussion

The reaction pathways investigated in this study are categorized into five different pathways, i.e., A, B, C, D, and E, shown in Figure 1. Each of the stationary points is labeled with a number in order to facilitate the discussion. The fully optimized geometries for those stationary points calculated at the B3LYP/6-31++G** level are given in Figures 2 and 3. The potential energy surfaces (PES) for the NCO + C_2H_2 reaction is presented in Figures 4 and 5 calculated at the CCSD(T)/6-31++G**//B3LYP/6-31++G** level. The calculated ground electronic energies and the relative energies of all the possible intermediates and the transition structures with respect to the reactants (NCO + C_2H_2) are listed in Tables 1 and 2. The various intermediates of the [C_2H_2NCO] complex are labeled from 1 to 13, and the possible final products, HCCO + HCN, HCCO + HNC, HNCO + C_2H, HOCN + C_2H, and HC_2NCO + H, are also labeled in order from P1 to P5. The symbol, TS_{i-j} stands for a transition species in connection with the two intermediates located at the local minima *i* and *j*.

Reaction NCO + C_2H_2 → HCCO + HCN (HNC). There are two possible pathways to form the oxazole intermediate, **3**, shown in Figure 1. One is the approach of the nitrogen atom of NCO to the carbon atom of acetylene to form complex **1** (energy barrier 3.49 kcal/mol (CCSD(T)), and the other is using the oxygen atom of NCO as an approach instead, and form complex **2** (17.97 kcal/mol (CCSD(T)). They may both further form the oxazole radical, a very stable intermediate complex about 19.23 kcal/mol less in energy than the starting species. However, the intermediate complex **1** locates at a much lower relative energy (−23.50 kcal/mol) than the complex **2** (+2.02 kcal/mol). The C−O bond and the C−C bonds are more stretched in the TS_{R-2}, and consequently, the barrier is much higher to form complex **2**. Furthermore, it takes 15.31 kcal/mol as the energy barrier for complex **2** to reach the transition state, TS_{2-3}, and leads to the oxazole formation, while it needs 35.06 kcal/mol for complex **1** to overcome the barrier, TS_{1-3}, leading to the same complex formation. As shown in the potential energy surfaces in Figure 4, it takes about 16.50 kcal/mol to break the C−O bond of oxazole and form the compound **4** (cis form) which is more stable than the starting species by 29.96 kcal/mol. It may go further by passing the barrier (TS_{4-5}, 9.75 kcal/mol) to form

TABLE 1: Ground-State Electronic Energies (au) and the Relative Energies (kcal/mol) of the Reactant, Intermediates, Transition States, and the Products for C_2H_2 + NCO/NCS → HCCO/HCCS + HCN(HNC) Reactions

	CCSD(T)/6-31++G**// B3LYP/6-31++G**				
species	E + ZPE [a]	$\Delta(E + \text{ZPE})$[b]	species	E + ZPE [a]	$\Delta(E + \text{ZPE})$[b]
(R)NCO + C_2H_2	−244.667664	0	(R_S)NCS + C_2H_2	−567.293121	0
1	−244.705117	−23.50	1s	−567.301036	−4.97
2	−244.664440	2.02	2s	−567.299232	−3.84
3	−244.698304	−19.23	3s	−567.328179	−22.00
4	−244.715409	−29.96	4s	−567.327905	−21.83
5	−244.717970	−31.57	5s	−567.330348	−23.36
6	−244.675888	−5.16	6s	−567.273080	12.58
7	−244.644767	14.37	7s	−567.245671	29.77
TS_{R-1}	−244.662108	3.49	TS_{R-1s}	−567.264930	17.69
TS_{R-2}	−244.639021	17.97	TS_{R-2s}	−567.283502	6.04
TS_{1-3}	−244.649235	11.56	TS_{1-3s}	−567.266390	16.77
TS_{2-3}	−244.639729	17.53	TS_{2-3s}	−567.274879	11.45
TS_{3-4}	−244.672070	−2.77	TS_{3-4s}	−567.301462	−5.23
TS_{4-5}	−244.699871	−20.21	TS_{4-5s}	−567.299745	−4.16
TS_{5-6}	−244.627668	25.08	TS_{5-6s}	−567.235515	36.15
TS_{6-7}	−244.591964	47.50	TS_{6-7s}	−567.191243	63.93
TS_{6-P1}	−244.660795	4.31	TS_{6-P1s}	−567.265228	17.50
TS_{7-P2}	−244.632157	22.28	TS_{7-P2s}	−567.233795	37.23
P1(HCN + HCCO)	−244.687739	−12.58	P1s (HCN + HCCS)	−567.301404	−5.20
P2(HNC + HCCO)	−244.664553	1.95	P2s (HNC + HCCS)	−567.278217	9.35

[a] The calculated ground electronic state energies of CCSD(T)/6-31++G**//B3LYP/6-31++G** with zero-point energy correction at B3LYP/6-31++G** level (au). [b] The relative energies of the species with respect to the reactant calculated at CCSD(T)/6-31++G**//B3LYP/6-31++G** level (kcal/mol).

TABLE 2: Ground State Electronic Energies (au) and the Relative Energies (kcal/mol) of the Reactant, Intermediates, Transition States, and the Products for C_2H_2 + NCO/NCS → C_2H + HNCO(HOCN)/HNCS(HOCN) or H + HC_2NCO/HC_2NCS Reactions

	CCSD(T)/6-31++G**// B3LYP/6-31++G**				
species	E + ZPE [a]	$\Delta(E + \text{ZPE})$[b]	species	E + ZPE [a]	$\Delta(E + \text{ZPE})$[b]
	HCCH + NCO → C_2H + HNCO(NCOH)/HNCS(HOCN)				
(R)NCO + C_2H_2	−244.667664	0	(R_S)NCS + C_2H_2	−567.293121	0
TS_{R-1}	−244.662108	3.49	2s	−567.299232	−3.84
1	−244.705117	−23.50	8s	−567.299378	−3.93
8	−244.705521	−23.76	9s	−567.216128	48.31
10	−244.716625	−30.72	10s	−567.305097	−7.52
13	−244.647861	12.42	11s	−567.269196	15.01
12	−244.687393	−12.38	12s	−567.230181	39.50
11	−244.619255	30.38	TS_{R-2s}	−567.283502	6.04
9	−244.581228	54.24	TS_{2-8s}	−567.297738	−2.90
TS_{1-8}	−244.703297	−22.36	TS_{2-9s}	−567.201936	57.22
TS_{8-10}	−244.630743	23.17	TS_{8-10s}	−567.228445	40.58
TS_{8-13}	−244.597896	43.78	TS_{8-11s}	−567.215807	48.51
TS_{8-11}	−244.57987	55.09	TS_{9-P3s}	−567.207629	53.65
TS_{1-9}	−244.581448	54.10	TS_{11-P3s}	−567.266583	38.53
TS_{10-13}	−244.627573	25.16	TS_{12-P4s}	−567.200618	58.05
TS_{10-12}	−244.584387	52.26	$TS_{RP4\,s}$	−567.235715	36.02
TS_{13-P4}	−244.588769	49.50	P3s(C_2H + HNCS)	−567.224121	43.30
TS_{12-P3}	−244.626305	25.95	P4s(C_2H + HSCN)	−567.215644	48.62
TS_{11-P3}	−244.606137	38.61			
TS_{9-P4}	−244.57002	61.27			
TS_{RP3}	−244.62301	28.02			
P3(C_2H + HNCO)	−244.632944	21.79			
P4(C_2H + HOCN)	−244.596486	44.67			
	HCCH + NCO/NCS → H + HC_2NCO/HC_2NCS				
TS_{8-P5}	−244.636288	21.03	TS_{8-P5s}	−567.226024	39.19
TS_{10-P5}	−244.634154	19.69	TS_{10-P5s}	−567.230672	42.10
P5(H + HC_2NCO)	−244.641822	16.21	P5s(H + HC_2NCS)	−567.237054	35.18

[a] The calculated ground electronic state energies of CCSD(T)/6-31++G**//B3LYP/6-31++G** with zero-point energy correction at B3LYP/6-31++G** level (au). [b] The relative energies of the species with respect to the reactant calculated at CCSD(T)/6-31++G**//B3LYP/6-31++G** level (kcal/mol).

compound **5** (trans form) which is even lower in energy than the cis form by 1.61 kcal/mol. To form the product P2 (HCN + HCCO) or P1 (HNC + HCCO), it is possible to initiate an intramolecular hydrogen transfer by crossing over a high energy barrier (56.65 kcal/mol, TS_{5-6}), and leads to an intermediate complex **6**. Then it may be either, by passing another high-energy barrier (52.66 kcal/mol, TS_{6-7}) to form **7**, or by passing a lower one (9.47 kcal/mol, TS_{6-P1}) to produce P1 (HCN + HCCO). The former process which passes the transition state TS_{6-7} may be followed by the breaking of the N−C bond (the N−C bond length in TS_{7-P2} is 1.840 Å) to produce P2 (HNC + HCCO), while in the latter process the N−C bond length in TS_{6-P1} is 1.854 Å, very similar to that in TS_{7-P2}. Comparing the energies of P1 and P2 in the potential energy surface, we found that HCN is more stable than HNC by 14.53 kcal/mol. The P1 formation channel is exothermic by 12.58 kcal/mol, and the net energy barrier is only 25.08 kcal/mol, much smaller than the P2 formation channel (47.50 kcal/mol, and slightly endot-

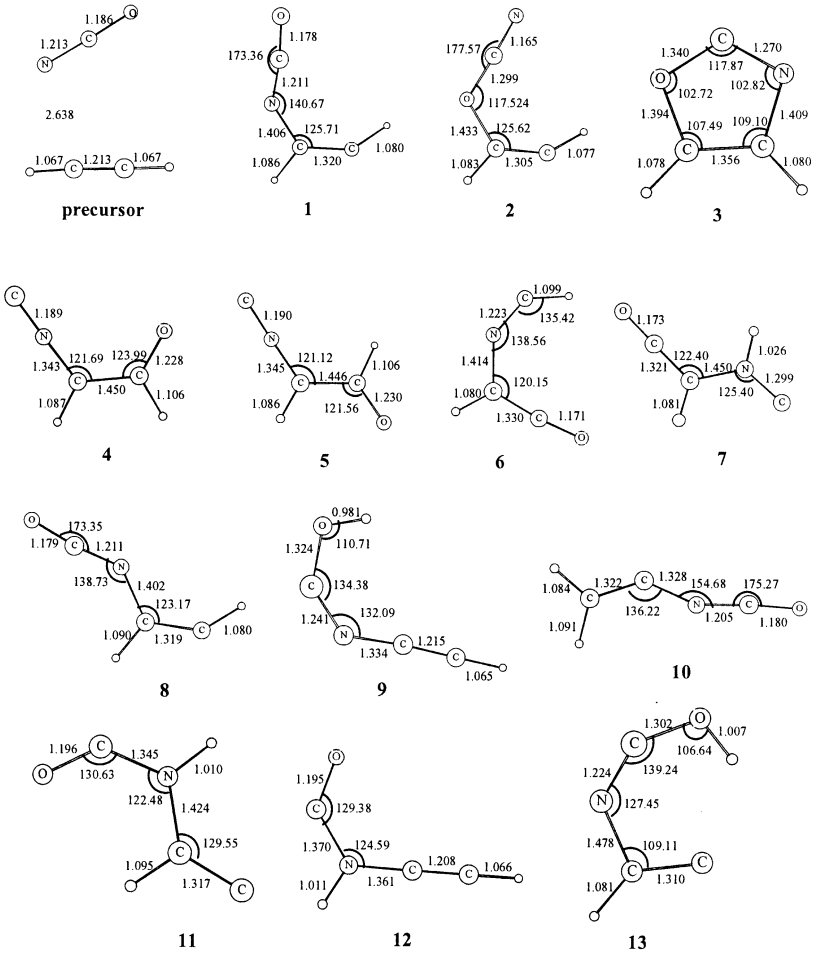

Figure 2. The optimized geometries of the possible intermediates (C_2H_2NCO) calculated at the B3LYP/6-31++G** level. Bond lengths are given in Å and angles in degrees.

hermic). Therefore, the P2 formation channel could be precluded. It agrees well with Wiesen et al.[20] who predicted that one of the lower product channels could be via the oxazole intermediate leading to P1 (HCN + HCCO) formation.

Reaction NCO + C_2H_2→ HNCO (NCOH) + C_2H. The calculated reaction barrier of direct hydrogen-abstraction is only 28.02 kcal/mol, TS_{RP3} (in Figure 3), which has the N−H bond length 1.071 Å, much longer than that in HNCO (1.008 Å). Also, it is endothermic of 21.79 kcal/mol (in Figure 5). There are two resonance structures of NCO, shown as below:

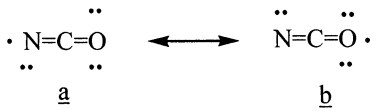

The DFT calculation showed that the atomic spin densities are N = 0.72 and O = 0.36. Therefore it is practical to adopt structure (*a*) as a standard bonding structure of NCO, and the direct hydrogen abstraction to form HNCO is thus more preferable. We also calculated the direct hydrogen abstraction from the other side of NCO to form NCOH + C_2H, yet the transition state for this pathway was not found. An alternative method to form NCOH + C_2H may be via the process of addition−elimination. The primary step was to form the intermediate complex **1** (refer to Figures 1 and 5), followed by a hydrogen transfer (transition structure TS_{1-9}, energy barrier 77.60 kcal/mol) and formed the intermediate **9**. Then, through the breaking of the N−C bond it led to the formation of P4 (via TS_{9-P4}, energy barrier 7.03 kcal/mol). It was endothermic of 44.67 kcal/mol. There were several other schemes via hydrogen transfer to produce products P3 (HNCO + C_2H) and P4 (HOCN + C_2H) from **8**, shown below. The energy barriers

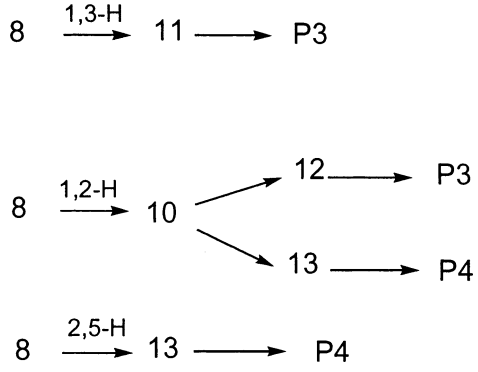

for these hydrogen transfer processes were quite high. As shown in Figure 5, it took 78.85 kcal/mol to pass the TS_{8-11} (via 1,3-H shift) to form **11**, followed by the breaking of N−C bond to produce P3 (HNCO + C_2H). The calculated bond-breaking barrier was 8.23 kcal/mol (TS_{11-P3}). However, the 1,2 H-shift from **8** may form a very stable conformer, **10**, 30.72 kcal/mol lower than the reactants, and the barrier for this transfer was 46.93 kcal/mol, TS_{8-10}. From our calculation it seemed unlikely to proceed further from **10** to produce P3 or P4, since it needed to form **12** or **13** first. The barriers of 82.98 and 55.88 kcal/mol for TS_{10-12}, and TS_{10-13}, respectively, were extremely high;

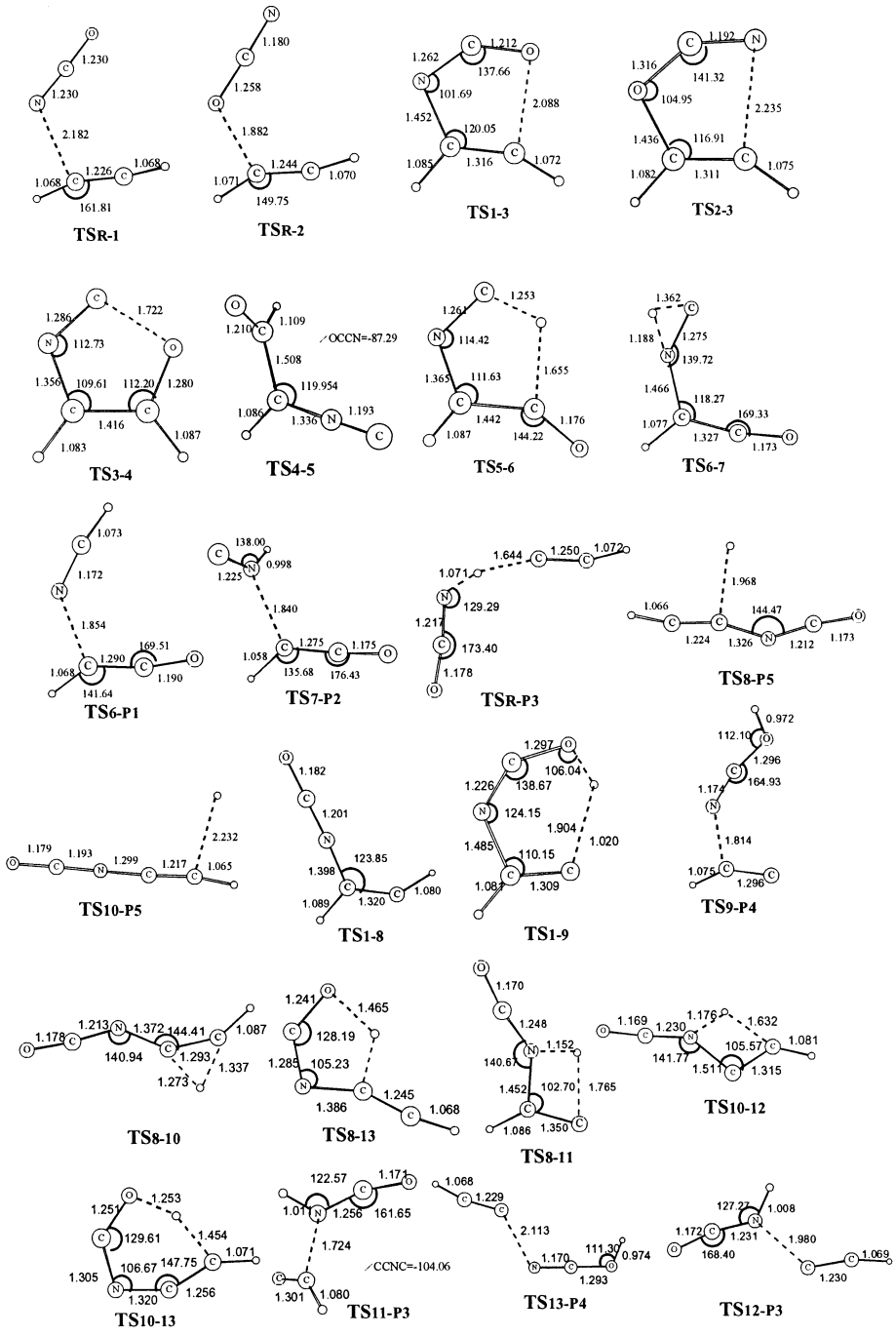

Figure 3. The optimized geometries of the transition structures (TS_{ij}) calculated at the B3LYP/6-31++G** level. Bond lengths are given in Å and angles in degrees.

then the following barriers 38.33 kcal/mol for **12** to form P3, and 37.08 kcal/mol for **13** to form P4, still needed to be overcome. Alternatively, complex **8** might form **13** via the 2,5-H shift, 67.54 kcal/mol through TS_{8-13}, then from **13** to P4 (37.08 kcal/mol for the barrier), a bit lower than the previous path.

Reaction of NCO + C_2H_2 → C_2HNCO + H. It is possible to break the C−H bond instead of the N−C bond to form P5 (C_2HNCO + H) from complexes **8** and **10**, and the energy barriers are 44.79 and 50.41 kcal/mol, respectively; whereas the barriers calculated from the reference point are only 21.03 kcal/mol (TS_{8-P5}) and 19.69 kcal/mol (TS_{10-P5}) by passing from **8** and **10**, respectively. Comparatively, they are not too high, and these two channels leading to P5 (H + HCCNCO) formation seem very likely. Incidentally, P5 formation was excluded by Wiesen et al.[20] because of their calculated high endothermic by around 28.95 kcal/mol. However, from our calculated barriers of this channel and the absorption of heat as low as 16.21 kcal/mol, we may agree with his prediction only if the reaction takes place at low temperature.

The isoelectronic species NCS may be an intermediate in the combustion of sulfur-containing fuels, yet not very many related reports for the reaction have previously appeared except the subject relating to NCS spectroscopic studies.[27] We presented our study of the reaction of NCS with C_2H_2 as a comparison with that of the NCO radical. Our calculated stable structures in the reaction of NCS + C_2H_2 are shown in Figure 6 and those of the transition structures in Figure 7. The notation underneath each structure is presented in a way similar to those in the NCO mechanistic processes, except by adding an "s" nearby each number to represent the NCS counterpart.

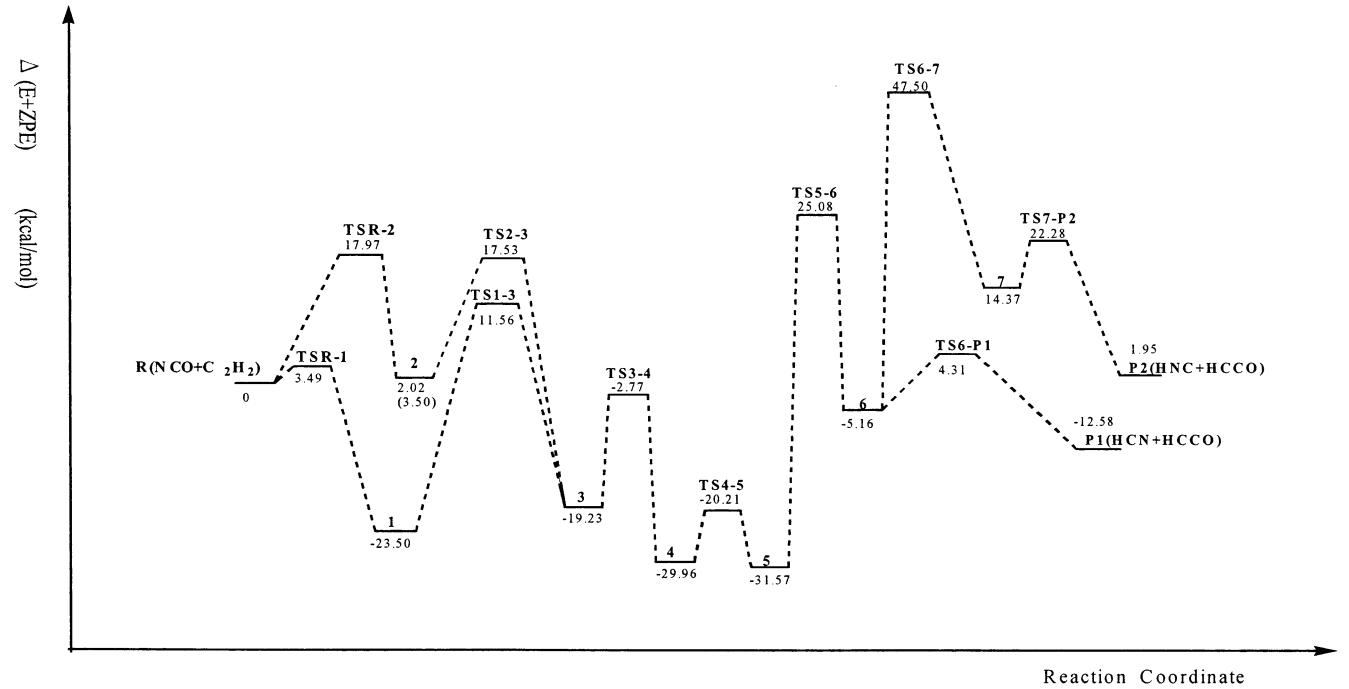

Figure 4. The potential energy surfaces for the pathways of the NCO + C_2H_2 reaction leading to the products P1 and P2, calculated at the CCSD(T)/6-31++G**//B3LYP/6-31++G** level with ZPE correction.

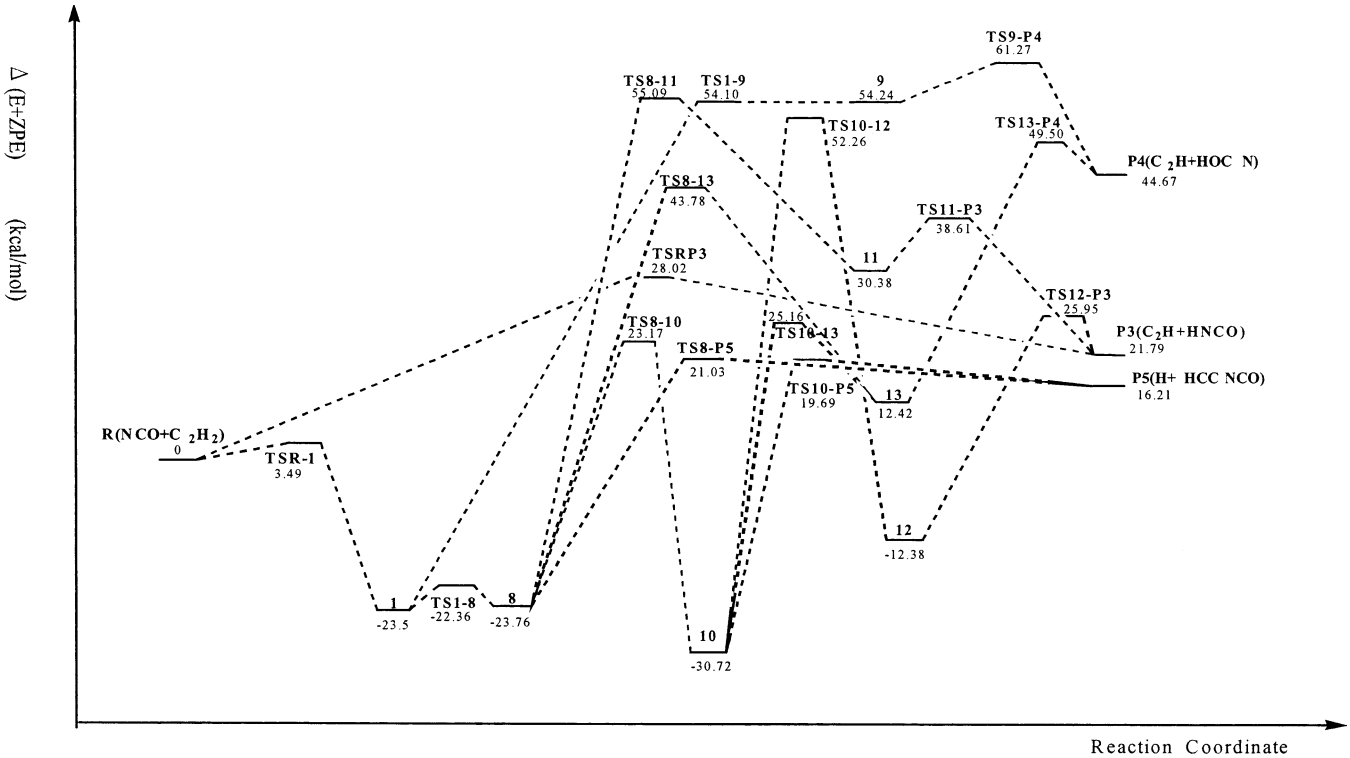

Figure 5. The potential energy surfaces for the pathways of the NCO + C_2H_2 reaction leading to the products P3, P4, and P5, calculated at the CCSD(T)/6-31++G**//B3LYP/6-31++G** level with ZPE correction.

Reaction of NCS + C_2H_2 → HCCS + HCN (HNC). The calculated ground electronic energies and the relative energies of all the possible intermediate structures with respect to the reactants (NCS + C_2H_2) are listed in Tables 1 and 2, and that of the potential energy surfaces for the reaction are not shown; however, they resemble those in Figures 4 and 5. Analogous to NCO, the reaction may initiate by applying the terminal atoms of the NCS to attack on the C_2H_2 and forms the **1s** or **2s**. Each then forms the intermediate complex **3s** (thiazole), afterward. We found that the S atom of NCS was much easier to perform the attack onto the C_2H_2 as compared to the N atom. It was quite opposite to that of the NCO counterpart, in which the N attack had a smaller barrier than the O barrier. The relative energy of the transition state TS_{R-2s} (6.04 kcal/mol) was much lower than that of TS_{R-1s} (17.69 kcal/mol) (refer to Figure 7 and Tables 1 and 2), so did the activation energies of the followed thiazole formation via TS_{2-3s} (about 6.45 kcal/mol smaller than via TS_{1-3s}). A reasonable explanation may be raised that the role of NCO (or NCS) in the reaction was more likely to act more as an electrophile than a nucleophile. As a

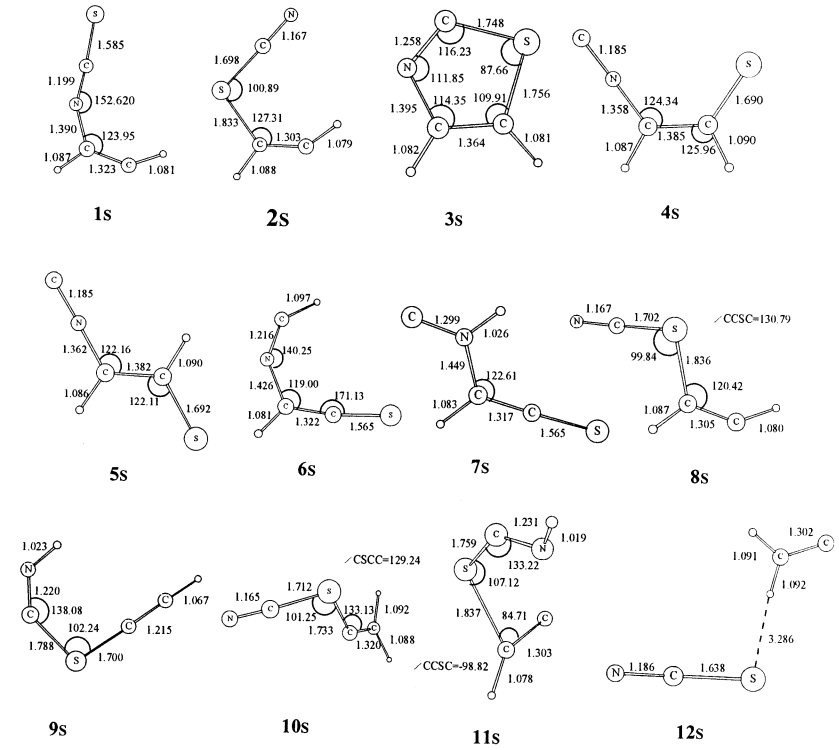

Figure 6. The optimized geometries of the possible intermediates (C_2H_2NCS) calculated at the B3LYP/6-31++G** level. Bond lengths are given in Å and angles in degrees.

consequence, the electronegativity of the terminal atom of NCO or NCS (N, O, and S) determined the ease for the site of the attack of NCO or NCS onto the C_2H_2. The weaker the electronegativity of the end atom, the easier it is for the atom to proceed to attack. Therefore, our calculated result agrees well with the above statement, since the sequential order of the electronegativity is O > N > S. The rest of the processes after the thiazole formation, such as the breakage of the C−S bond, and the migration of the H atom are similar to those of the NCO analogue, so do the activation energies of the corresponding processes. (For example, the breakage of the C−O or C−S bond is around 17 kcal/mol, and the migration of the hydrogen atom, **5** (or **5s**) → TS_{5-6} (or TS_{5-6s}) → **6** (or **6s**) is around 58 kcal/mol. However, the breakage of the C−N bond leading to the P1s formation (HCCS + HCN) is smaller in activation energy (∼5 kcal/mol) in the NCS as compared to the NCO counterpart (∼9 kcal/mol, P1 formation, HCCO + HCN). The isomerization processes from 6s to 7s and finally leading to the P2s formation (HCCS + HNC) also have similar activation energies as compared to the NCO analogue. From the calculated potential energy surfaces we know that the product formation of P1s (HCN + HCCS) is much more favored than the P2s (HNC + HCCS), similar to the NCO counterpart.

Reaction of NCS + C_2H_2 → C_2H + HSCN (HNCS). Unlike the NCO counterpart, the hydrogen abstraction of the NCS + C_2H_2 reaction yielded the product P4s (HSCN + C_2H) instead of HNCS + C_2H. It could be rationalized from the followings. There are two possible resonant structures of NCS drawn as follows:

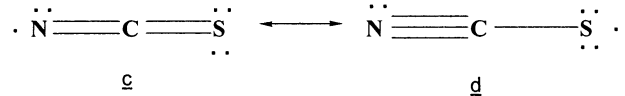

c d

From the calculated spin densities, N = 0.41 and S = 0.79, we believed that structure (*d*) could be a major conformer in which the unpaired electron was more likely to locate on the S atom. Therefore, the hydrogen abstraction reaction was expected to occur on the S atom to form the HSCN, with the barrier of 36.02 kcal/mol. Although there was no direct hydrogen abstraction pathway to form HNCS, it was possible to have HNCS formation via **2s** then through hydrogen shift to form **11s**, and finally broke the S−C bond and form the P3s product (HNCS + C_2H). The energy barrier for the hydrogen shift to overcome the transition state TS_{2-11s} was about 52 kcal/mol, and that of the dissociation of the S−C bond was about 23.5 kcal/mol. Obviously, the HSCN formation is more favored kinetically.

Reaction of NCS + C_2H_2 → C_2HSCN + H. The formation of stable complex **8s** may further dissociate one hydrogen atom to form theP5s product (H + HCCSCN) which locates at relative lower energies as compared to the P3s and P4s. The calculated energies and relative energies of the related species on the potential energy surface are listed in the lower part of Table 2. This direct stretch of the C−H bond needs about 43 kcal/mol to reach the barrier (TS_{8-P5s}), and then falls apart to form the P5s product. An alternative pathway leading to the same product was the dissociation of one hydrogen atom from complex **10s**. However, this barrier was much higher (49.62 kcal/mol) as compared to the former one. The mechanisms as well as the energy barriers of these two pathways were similar to those of the NCO counterpart.

Conclusion

We have used the DFT (B3LYP/6-31++G**) method and CCSD(T) single-point calculation based on the optimized geometry of B3LYP/6-31++G** to calculate the possible reaction pathways of C_2H_2 + NCO/NCS, as well as the energies of the local points and transition structures on the potential energy surfaces. Like NCO, the possible products for the NCS + C_2H_2 reaction are HCCS + HCN(HNC) (P1s and P2s), C_2H + HNCS(HSCN) (P3s and P4s), and H + HCCSCN (P5s). And the order of magnitude of the relative energies for these products

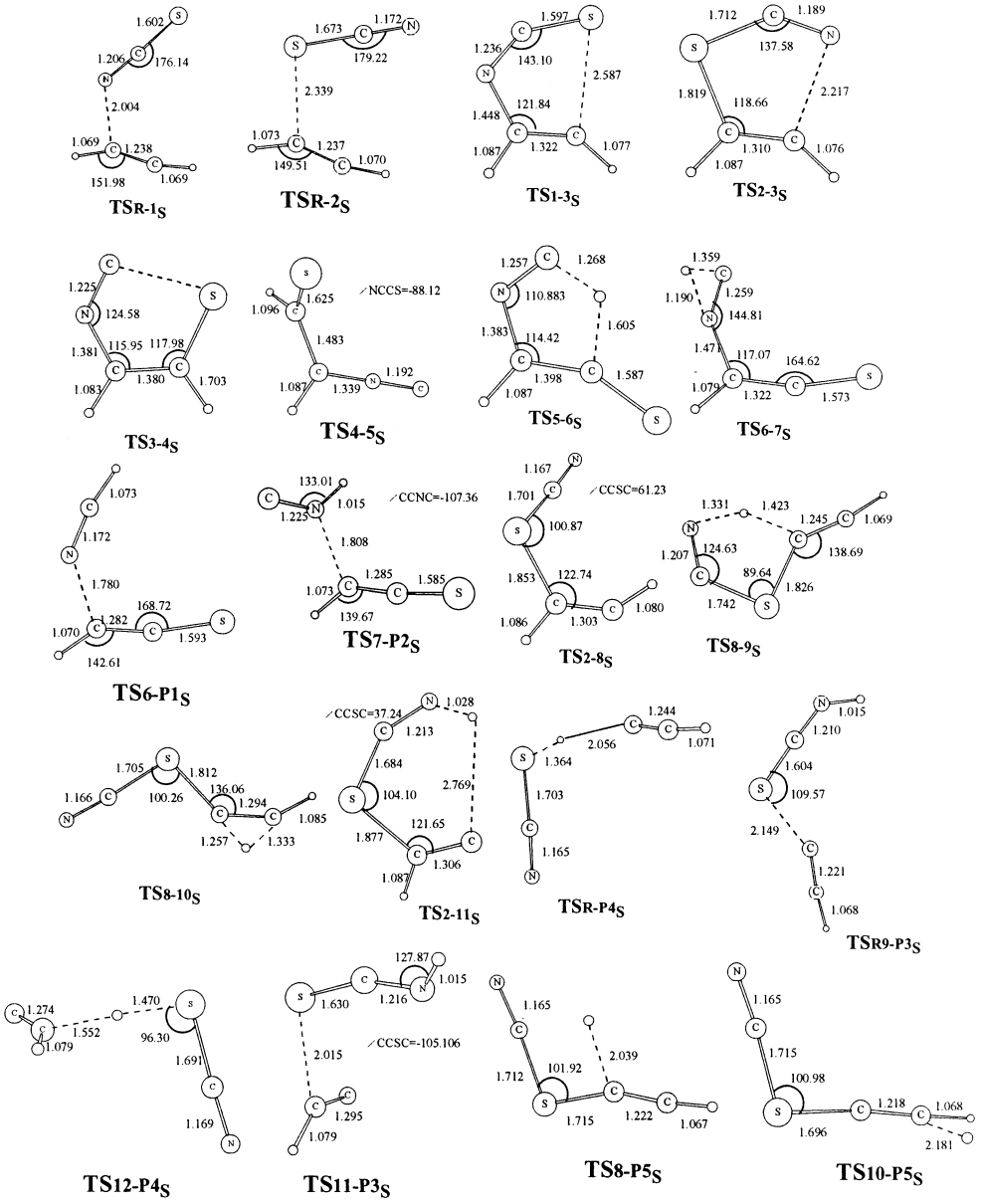

Figure 7. The optimized geometries of the transition structures (TS_{i-js}) calculated at the B3LYP/6-31++G** level. Bond lengths are given in Å and angles in degrees.

are similar, that is, P1 < P2 < P5 < P3 <P4; P1s < P2s < P5s < P3s < P4s. Unlike NCO, the formation of **2s** is more favored kinetically than that of **1s**, so does the formation of **3s** (thiazole) directly from **2s**. The spin contamination was not severe in all calculations (S^2 remains 0.75 in the B3LYP calculation, while it increases to 0.9 in the CCSD(T) single-point calculation). Thermal corrections and entropy are taken into account for NCO at five different temperatures ranging from 298 to 1200 K, and the results are listed in Table 3. The transition structures become destabilized to a different extent with the increased temperatures. However, the one with abstraction process, TS_{RP3}, is disturbed less, indicating the process would be enhanced at higher temperatures. Also the product channels P1 (HCN + HCCO), P3 (C_2H + HNCO), and P4 (C_2H + HOCN) are quite favored by the entropic component, since they are more stable at higher temperatures; in contrast to the P5 (H + HCCNCO) channel, it becomes less stable at higher temperatures. In all of the discussed pathways of C_2H_2 + NCO/NCS, the process leading to P3 (HNCO + C_2H)/P4s (HSCN + C_2H) were simple and direct, yet the calculated barriers were still high (28.02 kcal/mol, TS_{RP3}, and 36.02 kcal/mol, TS_{RP4s}), which would not occur at room temperature without an external energy booster. Incidentally, several experimental works[8,16,20] for measuring the rate coefficient of NCO + C_2H_2 showed quite split results ranging from $(7.47 \pm 0.8) \times 10^{-14}$, [16] $(1.10 \pm 0.02) \times 10^{-13}$, [20] to 1.90×10^{-13}, [8] by measuring the concentration change of different species in the reaction. The former performed a direct observation for the formation of HNCO, while the latter two measured the decay rate of NCO. Obviously, these diverse rate coefficients may represent different reaction pathways. However, the temperature dependence of rate coefficients for the direct observation of HNCO formation (from that we may know the activation energy experimentally) was not seen in the recent literature. Thus, whether the hydrogen abstraction process in forming HNCO could be a major product channel is still an open issue. Future experiments are clearly necessary to resolve this argument. The two pathways leading to P5 formation having lower overall barriers in the NCO case (21.03 kcal/mol via TS_{8-P5}, and 19.69 kcal/mol via TS_{10-P5}) involved more complexes formation (**1**, **8**, and **10**) though. The formation of P1

TABLE 3: The Relative Free Energies (kcal/mol) for the Reactant, Transition States, and Products at Five Different Temperatures Calculated at the CCSD(T)/6-31++G//B3LYP/6-31++G**Level**

	ΔG				
species	298.15 K	500 K	700 K	1000 K	1200 K
R (NCO + C_2H_2)	0.00	0.00	0.00	0.00	0.00
TS_{5-6}	33.47	40.10	46.86	57.04	63.79
TS_{6-7}	55.13	60.75	66.40	74.85	80.45
TS_{RP3}	33.85	37.89	41.91	47.89	51.85
TS_{13-4P}	55.20	58.89	62.54	68.02	71.67
TS_{8-5P}	28.51	33.74	38.86	46.43	51.41
P1(HCN + HCCO)	−13.79	−14.76	−15.71	−17.06	−17.92
P2(HNC + HCCO)	3.50	4.59	5.71	7.50	8.77
P3(C_2H + HNCO)	20.24	18.94	17.71	16.00	14.94
P4(C_2H + HOCN)	42.96	41.52	40.14	38.22	37.03
P5(H + HCCNCO)	21.96	25.33	28.50	33.00	35.90
R (NCS + C_2H_2)	0.00	0.00	0.00	0.00	0.00
TS_{5-6s}	44.66	51.46	58.42	68.88	75.83
TS_{6-7s}	71.52	77.13	82.78	91.24	96.84
TS_{RP4s}	41.23	44.54	47.80	52.62	55.81
TS_{2-11s}	58.01	63.80	69.61	78.29	84.06
TS_{8-5Ps}	46.71	51.68	56.50	63.54	68.15
P1s(HCN + HCCS)	−5.61	−5.98	−6.38	−6.98	−7.38
P2s(HNC + HCCS)	11.68	13.37	15.04	17.58	19.31
P3s(C_2H + HNCS)	41.87	40.67	39.52	37.92	36.92
P4s(C_2H + HSCN)	46.67	45.06	43.50	41.27	39.85
P5s(H + HCCSCN)	36.87	37.41	37.68	37.79	37.73

(HCCO + HCN)/P1s (HCCS + HCN) was supported by the experimental prediction [20] that the short-lifetime OCN/SCN−C_2H_2 adducts were formed first and then undergo rapid transformation into the products.

Acknowledgment. We are indebted to the reviewers for their valuable suggestions concerning the manuscript. Support for this research from the National Science Council of the Republic of China (NSC-90-2113-M-003-014) is gratefully acknowledged. We are also grateful to the National Center for High-Performance Computing where the Gaussian package and the computer time were provided.

References and Notes

(1) Miller, J. A.; Bowman, C. T. *Prog. Energy Combust. Sci.* **1989**, *15*, 287.
(2) Perry, R. A. *J. Chem. Phys*. **1985**, *82*, 5485.
(3) Hancock, G.; McKendrick, K. G. *Chem. Phys. Lett.* **1986**, *127*, 125.
(4) Jones, W. E.; Wang, L. *Can. J. Appl. Spectrosc*. **1993**, *38*, 32.
(5) Atakan, B.; Wolfrum, J. *Chem. Phys. Lett*. **1991**, *178*, 157.
(6) Mertens, J. D.; Dean, A. J.; Hanson, R. K.; Bowman, C. T. *Symp. (Int.) Combust. Proc.* **1992**, *24*, 701.
(7) Juang, D. Y.; Lee, J.-S.; Wang, N. S. *Int. J. Chem. Kinet*. **1995**, *27*, 1111.
(8) Wategaonkar, S.; Setser, D. W. *J. Phys. Chem*. **1993**, *97*, 10028.
(9) Cooper, W. F.; Hershberger, J. F. *J. Phys. Chem.* **1992**, *96*, 771.
(10) Cooper, W. F.; Park, J.; Hershberger, J. F. *J. Phys. Chem*. **1993**, *97*, 3283.
(11) Park, J.; Hershberger, J. F. *J. Phys. Chem*. **1993**, *97*, 13647.
(12) Wooldridge, S. T.; Mertens, J. D.; Hanson, R. K.; Bowman, C. T. *Symp. (Int.) Combust. Proc.* **1994**, *25*, 983.
(13) Lin, M. C.; Rongshun, Z. *J. Phys. Chem A* **2000**, *104* (46), 10807−10811.
(14) Campomanes, P.; Menéndez, I.; Sordo, T. L. *J. Phys. Chem A* **2001**, *105*, 229−237.
(15) Perry, R. A. *Symp. (Int.) Combust. Proc*. **1986**, *25*, 913.
(16) Park, J.; Hershberger, J. F. *Chem. Phys. Lett*. **1994**, *218*, 537.
(17) Perry, R. A. *Symp. (Int.) Combust*. **1986,** *25*, 913.
(18) Schuck, A.; Volpp, H.-R.; Wolfrum, J. *Combust. Flame* **1994**, *99*, 491.
(19) Becker, K. H.; Kurtenbach, R.; Wiesen, P. *J. Phys. Chem.* **1995**, *99*, 5986.
(20) Becker, K. H.; Kurtenbach, R.; Schmidt, F.; Wiesen, P. *Chem. Phys. Lett*. **1995**, *235*, 230.
(21) Frisch, M. J.; Trucks, G. W.; Schlegel, H. B.; Scuseria, G. E.; Robb, M. A.; Cheeseman, J. R.; Zakrzewski, V. G.; Montgomery, J. A.; Stratmann, R. E., Jr.; Burant, J. C.; Dapprich, S.; Millam, J. M.; Daniels, A. D.; Kudin, K. N.; Strain, M. C.; Farkas, O.; Tomasi, J.; Barone, V.; Cossi, M.; Cammi, R.; Mennucci, B.; Pomelli, C.; Adamo, C.; Clifford, S.; Ochterski, J.; Petersson, G. A.; Ayala, P. Y.; Cui, Q.; Morokuma, K.; Malick, D. K.; Rabuck, A. D.; Raghavachari, K.; Foresman, J. B.; Cioslowski, J.; Ortiz, J. V.; Stefanov, B. B.; Liu, G.; Liashenko, A.; Piskorz, P.; Komaromi, I.; Gomperts, R.; Martin, R. L.; Fox, D. J.; Keith, T.; Al-Laham, M. A.; Peng, C. Y.; Nanayakkara, A.; Gonzalez, C.; Challacombe, M.; Gill, P. M. W.; Johnson, B.; Chen, W.; Wong, M. W.; Andres, J. L.; Gonzalez, C.; Head-Gordon, M.; Replogle, E. S.; Pople, J. A. *Gaussian 98, Revision A.6*; Gaussian, Inc.: Pittsburgh, PA, 1998.
(22) Becke, A. D. *J. Chem. Phys.* **1993**, *98*, 5648. (b) Becke, A. D. *J. Chem. Phys.* **1992**, *96*, 2155. (c) Becke, A. D. *J. Chem. Phys.* **1992**, *97*, 9173.
(23) Lee, C.; Yang, W.; Parr, R. G. *Phys. Rev.* **1988**, *B37*, 785.
(24) Gonzalez, C.; Schlegel, H. B. *J. Phys. Chem.* **1989**, *90*, 2154.
(25) Lee, T. J.; Scuseria, G. In *Quantum Mechanical Electronic Structure Calculations with Chemical Accuracy*; Langnoff, S. F., Ed.; Kluwer Academic Press: Dordrecht, The Netherlands, 1995.
(26) Becker, K. H.; Geiger, H.; Schmidt, F.; Wiesen, P. *Phys. Chem. Chem. Phys.* **1999**, *1*, 5305−5309.
(27) Baren, R. E.; Hershberger, J. F. *J. Phys. Chem. A* **1999**, *103*, 11340−11344.